

Preparation of Ni Aluminide/Ni Bilayer Coating on Nb–W Alloys by Molten Salt Electrodeposition and Oxidation Resistance

Naka Sato¹ · Masahiko Fuji¹ · Naoya Kohiruimaki¹ ·
Michihisa Fukumoto¹ · Motoi Hara¹

Received: 23 June 2015 / Published online: 21 July 2015
© Springer Science+Business Media New York 2015

Abstract Coatings consisting of Ni aluminide/Ni bilayer on Nb–W and Nb–W–Mo alloys were prepared by the electrodeposition of Al using a molten salt electrolyte after the Ni electrodeposition. The coating specimen with a thin Ni layer showed a vigorous oxidation during the initial period. On the contrary, the coating specimen with a thick Ni layer showed a high oxidation resistance. For the coating specimen with a thick Ni layer, a surface layer consisting of NiAl was formed after the oxidation test. For this coating specimen, further, intermediate layers consisting of Ni–Nb alloys were formed by the diffusion of the Ni layer and the alloy substrate during the oxidation test. These intermediate layers contributed to the maintenance of a high concentration of Al in the surface layer and the suppression of spallation of the surface layers, leading to the improvement in the oxidation resistance of the coating.

Keywords Electrodeposition · Molten salt · Aluminum · Niobium-base alloy · Oxidation · Coating · Nickel aluminide

Introduction

Nb-base alloys are promising materials for high temperature equipment because of their high melting point and high specific strength at high temperature. However, they have a very poor oxidation resistance above 973 K due to the inability of the

✉ Naka Sato
satonaka@ipc.akita-u.ac.jp
Motoi Hara
hara@ipc.akita-u.ac.jp

¹ Department of Materials Science and Engineering, Graduate School of Engineering and Resource, Akita University, Akita 010-8502, Japan

Nb-oxide scale that forms on the surface to provide any oxidation protection. As a result, the use of the Nb-base alloys at high temperature is severely restricted.

In order to improve the oxidation resistance of Nb-base alloys, the investigation about coatings of a high oxidation-resistant material onto a pure Nb or Nb-base alloy has been undertaken [1–3]. Matsubara et al. [1] performed the preparation of a coating consisting of $\text{Al}_2\text{O}_3\text{--MoSi}_2$ using the plasma spraying method and showed that the coating had a relatively high oxidation resistance. Murakami et al. [2] succeeded in the preparation of a coating consisting of $\text{Nb}_3\text{Si}_5\text{Al}_2$ using the spark plasma sintering method and showed that the adhesion of the coating to the substrate alloy was high. Matsumura et al. [3] succeeded in the preparation of a coating consisting of Ni-aluminide with a diffusion barrier against inward-Al diffusion by the electroplating of a Re–Ni film, Cr-pack cementation, Ni plating, and Al-pack cementation.

On the other hand, we have succeeded in the preparation of a coating consisting of Ni-aluminide on a Ni-base alloy [4], TiAl [5] and stainless steel [6] by Ni electrodeposition in an aqueous solution, followed by Al electrodeposition in a molten salt. We also have indicated that the oxidation resistance of the alloys was significantly improved by the coating consisting of Ni-aluminide.

In the present study, it was attempted to form a Ni-aluminide layer on Nb–W and Nb–W–Mo alloys, which are promising materials for high temperature equipment, by the electrodeposition of Ni and that of Al which can be electrodeposited using a molten salt as the electrolyte. When the formation of the Ni-aluminide was carried out by the Ni electrodeposition for a long time, followed by the Al electrodeposition, a Ni layer as the intermediate layer between the Ni-aluminide layer and the alloy substrate was formed. In the present study, we tried to prepare the Ni-aluminide/Ni bilayer coating by the Ni electrodeposition for a long time, followed by the Al electrodeposition. For the specimens with this coating, the oxidation resistance was evaluated.

Experimental Procedures

Nb-10 mass%W and Nb-10 mass%W-5 mass%Mo alloys were used as the cathode substrate. The alloy ingot was prepared by argon-arc melting. Coupons about 1.5-mm thick were cut from the ingot. The sample surface was polished with #800 SiC paper and ultrasonically washed in acetone.

The preparation of the Ni aluminide/Ni bilayer coatings were carried out in two electrodeposition steps. First, Ni was electrodeposited on the alloys using a Watt's solution. Second, Al was electrodeposited on the Ni film using an equimolar NaCl–KCl melt at 1023 K containing 3.5 mol% AlF_3 . The Ni-deposition time was changed in order to change the thickness of the Ni layer. The electrodeposition of Ni was carried out by galvanostatic electrolysis at 200 A m^{-2} for 3.6, 7.2, 10.8 and 12.6 ks. The electrodeposition of Al was carried out by potentiostatic electrolysis at -1.4 V (vs. $\text{Ag}/\text{AgCl}(0.1)$) for 3.6 ks.

The high-temperature oxidation test of the samples treated with the Ni and Al depositions was carried out at 1273 K in air for 259.2 ks using a thermobalance. In

order to evaluate the change in the coating layer and the scale formed on the coating layer after the oxidation test, a cross-section of the specimen was observed by SEM and analyzed by EPMA.

Results and Discussion

Morphology of Ni-aluminide/Ni Bilayer Coating

Figure 1 shows cross-sectional micrographs and the concentration profiles of the Al, Ni, Nb and W across the Nb-10 mass%W alloys after the Ni electrodeposition for 3.6–12.6 ks, followed by the Al electrodeposition. For each specimen, the formation of a uniform coating layer consisting of the outer and inner layers was observed. It was found from the concentration profiles that the outer and inner layers consisted of Ni_2Al_3 and Ni, respectively. At the interface between the Ni layer and the alloy substrate, the formation of a thin layer consisting of a Nb–Ni–W alloy was observed. The thickness of the Ni layer increased with an increase in the Ni electrodeposition time. Such a Ni_2Al_3 /Ni bilayer was also observed for the Nb-10 mass%W-5 mass%Mo alloy after the same Ni electrodeposition, followed by the Al electrodeposition.

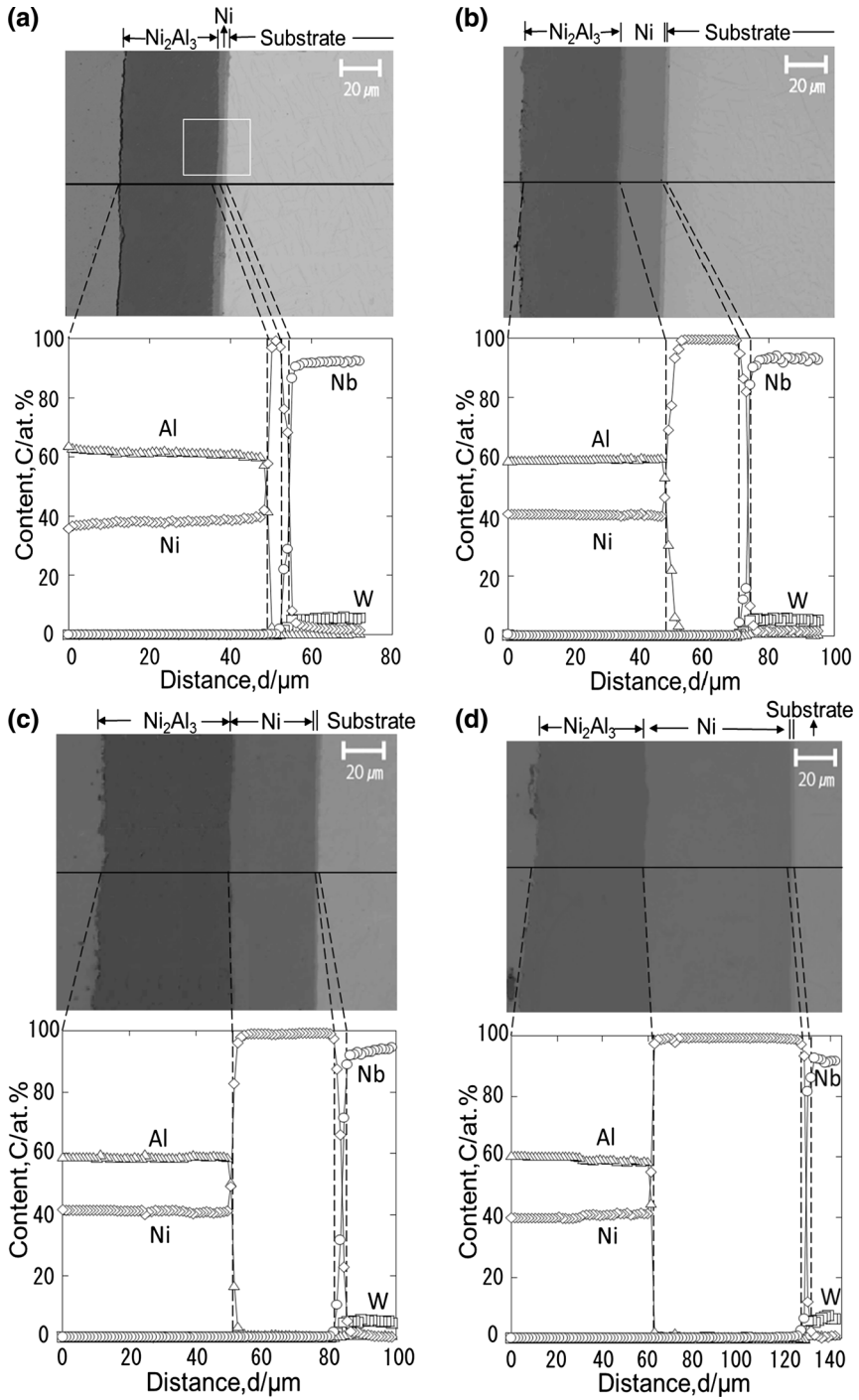
Figure 2 shows a cross-section micrograph and the concentration profiles of Al, Ni, Nb and W across an area at the interface between the Ni layer and the alloy substrate for the sample shown in Fig. 1a. It was found that a thin layer consisting of a Nb–Ni–W alloy was formed. It was presumed from the concentration profiles that this alloy consisted of NbNi_3 containing a small amount of W.

Oxidation Behavior at High Temperature

Figure 3a, b show the oxidation curves of the Nb-10 mass%W and Nb-10 mass%W-5 mass%Mo alloys, respectively, after the Ni electrodeposition for 3.6–12.6 ks, followed by the Al electrodeposition, during the oxidation test in air at 1273 K. This figure also contains the oxidation curve of a non-treated alloy in the same atmosphere. For both alloys with the coating formed by the Ni electrodeposition for 3.6 ks, the mass gains largely increased during the initial period due to a vigorous oxidation. On the contrary, for both alloys with the coatings formed by the Ni electrodeposition for a time longer than 7.2 ks, the mass gains were scarcely observed, showing that these specimens had a high oxidation resistance.

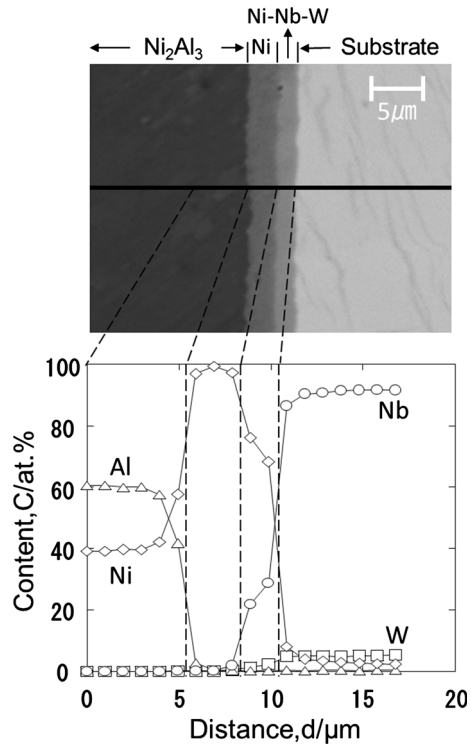
Morphology of Coating and Scale after Oxidation Test

Figure 4 shows a cross-sectional micrograph and the concentration profiles of Al, Ni, Nb, W and O across the Nb-10 mass%W alloy after the Ni electrodeposition for 3.6 ks, followed by the Al electrodeposition, after the oxidation for 3.6 ks at 1273 K in air. For this specimen, vigorous oxidation occurred during the initial period (Fig. 2). This micrograph was taken for the area in which the coating adhered to the alloy substrate. The coating consisted of Ni_2Al_3 as same as the outer layer before the



◀ **Fig. 1** Cross-sectional micrographs and concentration profiles of Nb, W, Al and Ni across Nb-10 mass%W alloy after Ni electrodeposition for **a** 3.6 ks, **b** 7.2 ks, **c** 10.8 ks, **d** 12.6 ks, and Al electrodeposition

Fig. 2 Cross-sectional micrographs and concentration profiles of Nb, W, Al and Ni across the area shown in the white frame in Fig. 1a



oxidation test. A scale consisting of Al_2O_3 was formed on the coating. At the interface between the coating and the alloy substrate, a thin layer consisting of the Ni–Nb–W alloy was formed. It was found that at the interface between the Ni–Nb–W alloy layer and the Ni_2Al_3 layer, spallation of the Ni_2Al_3 layer partly occurred. In the Ni_2Al_3 layer, cracks lying perpendicular to the surface were observed. It was presumed that such a spallation and cracks took place due to the thermal stress generated by the rise and fall in temperature before and after the oxidation test, which was caused by the difference in the expansion coefficient between the Ni_2Al_3 layer and the Ni-10 mass%W alloy substrate. Consequently, the large oxidation mass gain observed for the alloy after the Ni electrodeposition for 3.6 ks seems to result from the spallation of the Ni_2Al_3 layer, which was caused during the rise in the temperature before the oxidation test.

Figure 5a, b show cross-sectional micrographs and the concentration profiles of Al, Ni, Nb, W and O across the Nb-10 mass%W alloys after the Ni electrodeposition for 7.2 and 12.6 ks, respectively, followed by the Al electrodeposition, after the oxidation for 259.2 ks at 1273 K in air. These specimens showed a high oxidation resistance (Fig. 3). For the alloy with the coating formed by the Ni

electrodeposition for 7.2 ks (Fig. 5a), the outer layer changed from the Ni_2Al_3 phase to the NiAl phase after the oxidation due to a decrease in the Al concentration. It was presumed from the concentration profiles in the coating and the Ni–Al–Nb

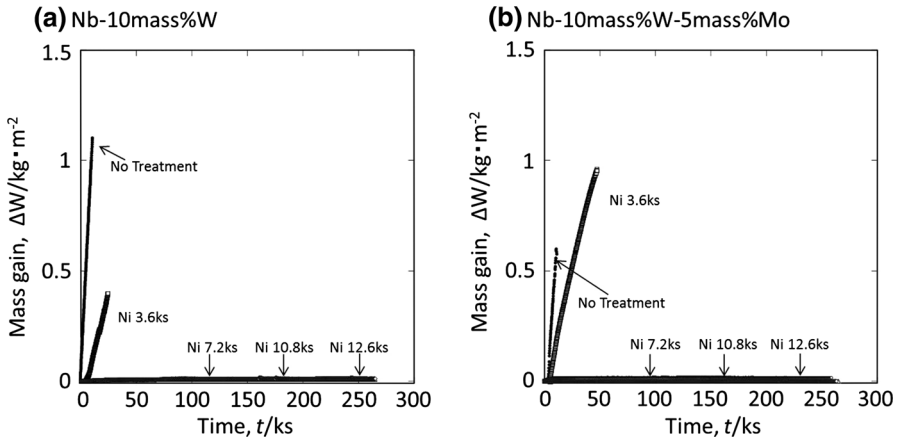
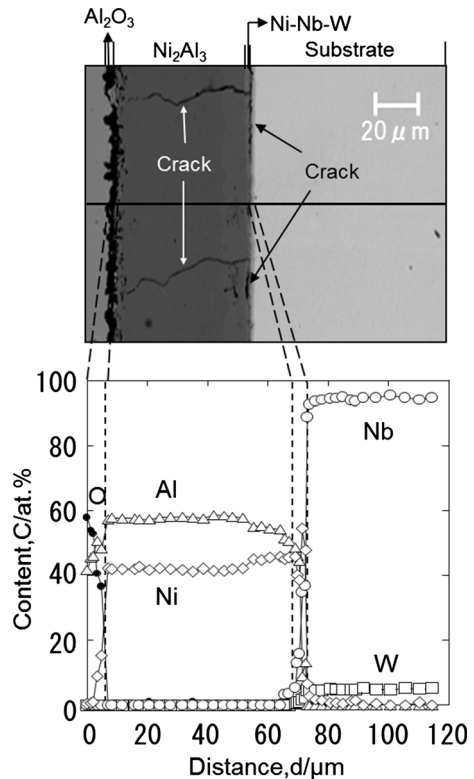


Fig. 3 Mass gain-time curves of **a** Nb-10 mass%W and **b** Nb-10 mass%W-5 mass%Mo alloy specimens, deposited with Al after Ni electrodeposition for 3.6–12.6 ks, during oxidation at 1273 K in air

Fig. 4 Cross-sectional micrographs and concentration profiles of Nb, W, Al and Ni across Nb-10 mass%W alloy deposited with Al after Ni electrodeposition for 3.6 ks, after oxidation for 3.6 ks at 1273 K in air



ternary diagram [7] that the inner Ni layer before the oxidation test reacted with the outer Ni_2Al_3 layer to form a NiAl layer and a layer consisting of NiAl and Ni_3Al , and the latter layer reacted with the alloy substrate to form a Nb_7Ni_6 layer and a layer consisting of Nb_7Ni_6 and a Nb-solid solution phase containing Ni. On the other hand, for the alloy with the coating formed by the Ni electrodeposition for 12.6 ks (Fig. 5b), it was presumed that the coating consisted of an outer NiAl layer and an inner Ni_3Al layer/a layer consisting of Ni_3Al and a Ni-solid solution phase containing Al/a layer consisting of a Ni-solid solution phase containing Nb/a layer consisting of NbNi_3 and Nb_7Ni_6 /a layer consisting of Nb_7Ni_6 and a Nb-solid solution phase containing Ni. It was found that corresponding to such a gradual change in the phase, the concentration of Al gradually decreased with a change in place from the coating surface to the alloy substrate. For both specimens shown in Fig. 5a, b, scales consisting of Al_2O_3 were formed on the outer NiAl layers. It was also found for both specimens that the area inside the layer consisting of the Nb_7Ni_6 phase scarcely contained Al, suggesting that this layer seems to inhibit the inward diffusion of Al.

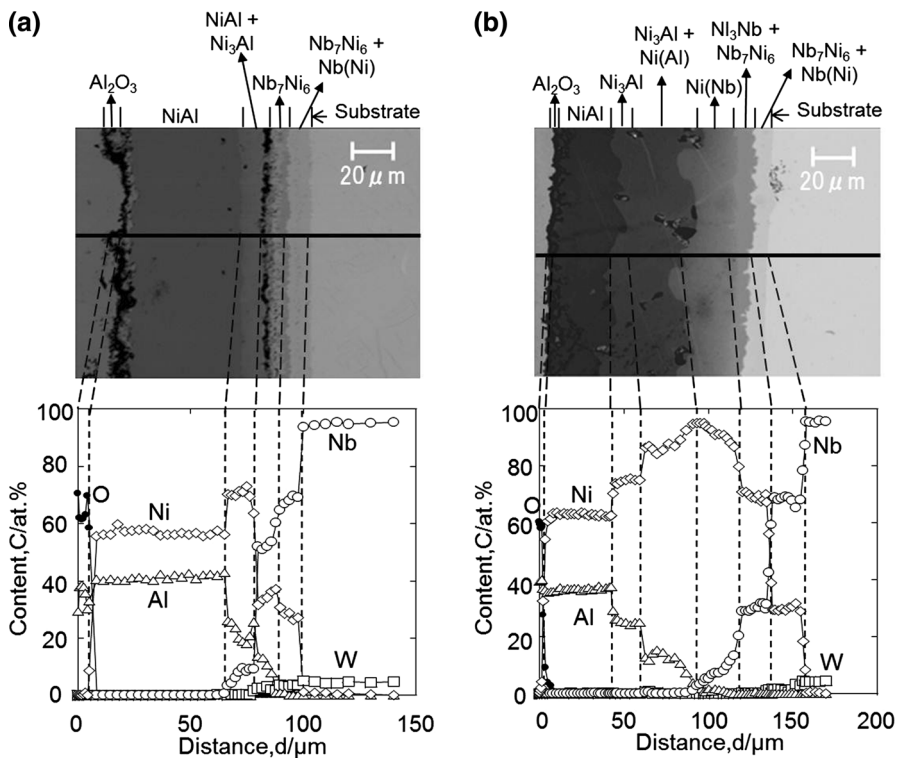


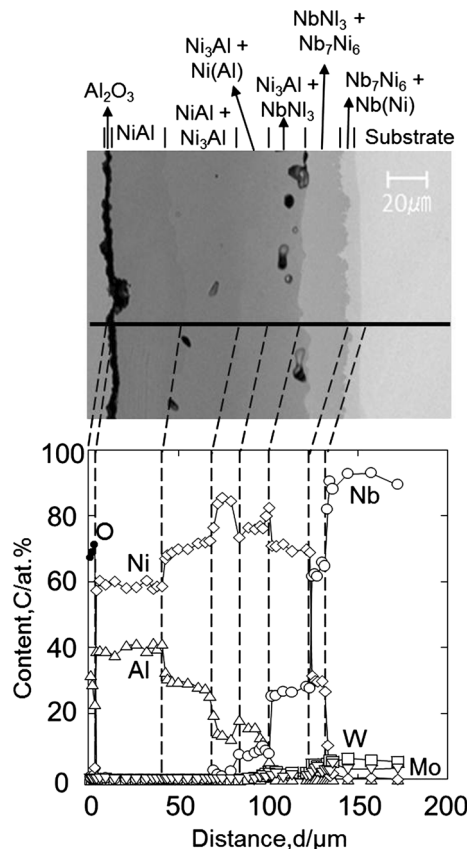
Fig. 5 Cross-sectional micrographs and concentration profiles of Nb, W, Al and Ni across Nb-10 mass%W alloy deposited with Al after Ni electrodeposition for **a** 7.2 ks and **b** 12.6 ks, after oxidation for 259.2 ks at 1273 K in air

Figure 6 shows cross-sectional micrographs and the concentration profiles of Al, Ni, Nb, W, Mo and O across the Nb-10 mass%W-5 mass%Mo alloy after the Ni electrodeposition for 12.6 ks, followed by the Al electrodeposition, after the oxidation for 259.2 ks at 1273 K in air. This specimen showed a high oxidation resistance (Fig. 3). It was presumed that the coating consisted of an outer NiAl layer and an inner layer consisting of NiAl and Ni₃Al/a layer of Ni₃Al and a Ni-solid solution phase containing Al/a layer consisting of Ni₃Al and NbNi₃/a layer consisting of NbNi₃ and Nb₇Ni₆/a layer consisting of Nb₇Ni₆ and a Nb-solid solution phase containing Ni. Such a tilting morphology of the coating was the same as that of the Nb-10 mass%W alloys after the Ni electrodeposition for 12.6 ks, followed by the Al electrodeposition, after the oxidation test (Fig. 5b). It was also found that on the outer NiAl layer, a scale consisting of Al₂O₃ had formed.

Effect of Ni Layer Thickness on Oxidation Behavior

Based on the results of this study that for Ni-10 mass%W and Ni-10 mass%W-5 mass%Mo alloy substrates, the formation of the thick Ni layer as an intermediate

Fig. 6 Cross-sectional micrographs and concentration profiles of Nb, W, Mo, Al and Ni across Nb-10 mass%W-5 mass%Mo alloy deposited with Al after Ni electrodeposition for 12.6 ks, after oxidation for 259.2 ks at 1273 K in air



layer led to the improvement of the oxidation resistance. This fact results from two factors. One factor is that the Al concentration in the outer layer was maintained at a high concentration due to the formation of the intermediate layer consisting of the Nb_7Ni_6 phase, which seems to inhibit the inward diffusion of Al. The other factor is that the generation of the crack at the interface between the coating and the alloy substrate due to the thermal stress during the temperature increase was depressed when the inner Ni layer was thick. Figure 7 shows the composition path for the coating formed on the Nb-10 mass%W alloys after the Ni electrodeposition for 7.2 and 12.6 ks, followed by the Al electrodeposition, after the oxidation test (Fig. 5a, b), in the Nb–Al–Ni system phase diagram at 1300 K [7]. For the coating formed on the Nb-10 mass%W alloy after the Ni electrodeposition for 7.2 ks (Fig. 5a), the number of passing phases after starting from the outer NiAl layer is three. On the contrary, for the coating formed on the Nb-10 mass%W alloy after the Ni electrodeposition for 12.6 ks (Fig. 5b), the number of the passing phases after starting from the outer NiAl layer is six. This indicated that the formation of the thick Ni layer led to the formation of the numerous layers having a variable chemical composition after the oxidation test. The fact seems to lead to a decrease in the thermal stress, which occurs on each layer constituting the coating during a change in temperature, thus suppressing spallation of the coating.

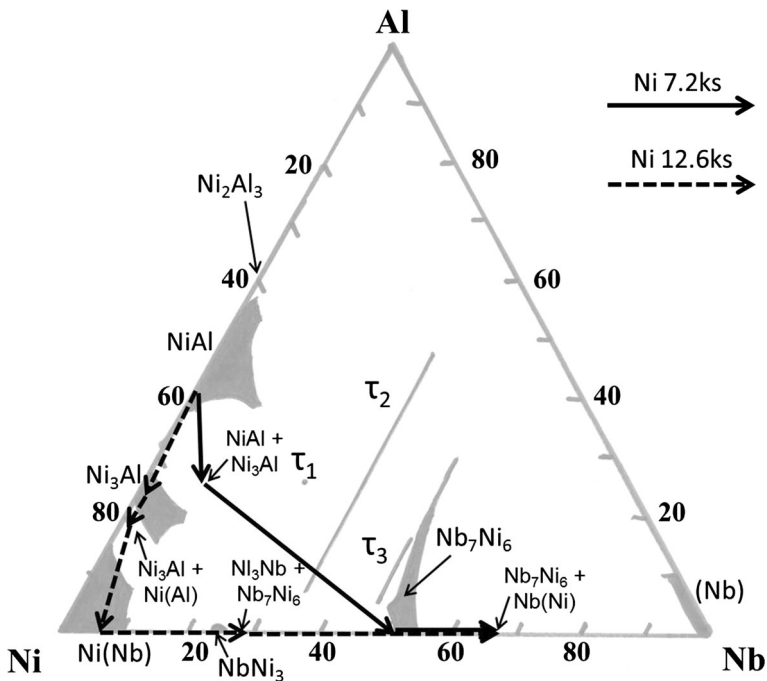


Fig. 7 Composition path for the Nb-10 mass%W alloys after Ni electrodeposition for 7.2 and 12.6 ks, followed by the Al electrodeposition after the oxidation test in the Nb–Al–Ni system phase (isothermal section at 1300 K)

Conclusions

The preparation of a Ni-aluminide/Ni bilayer coating on the Nb-10 mass%W and Nb-10 mass%W-5 mass%Mo alloys was attempted by Ni electrodeposition using an aqueous solution and Al electrodeposition using a molten salt. The oxidation resistance of the alloys with this coating was evaluated. The following conclusions can be drawn.

- (1) For the alloys treated with Ni-deposition in a Watt's solution, followed by Al-deposition in the molten salt, a coating consisting of a Ni-aluminide/Ni bilayer was formed. An inner Ni layer became thick with an increase in the Ni-deposition time.
- (2) The alloys with a coating consisting of a Ni-aluminide/thin Ni layer (Ni-deposition time; 3.6 ks) showed a vigorous oxidation during the initial period, while the alloys with a coating consisting of a Ni-aluminide/thick Ni layer (Ni-deposition time; longer than 7.2 ks) showed a high oxidation resistance.
- (3) For the alloys with a coating consisting of a Ni-aluminide/thick Ni layer showing a high oxidation resistance, several intermediate layers consisting of Ni–Al and Ni–Nb alloys were formed between the outer NiAl layer and the substrate alloy.

References

1. M. Matsudara and S. Hanada, *Journal of the Japan Institute of Metals* **63**, 112 (1999).
2. T. Murakami, S. Sasaki, K. Ichikawa, A. Kitahara, K. Ito, H. Inui and M. Yamaguchi, in *Structural Intermetallics*, vol. 581, eds. K. J. Hemker, D. M. Dimiduk, H. Clemens, R. Darolia, H. Inui, J. M. Larsen, V. K. Sikka, M. Thomas and J. D. Whittenberger (TMS, Warrendale, 2001).
3. Y. Matsumura, M. Fukumoto, S. Hayashi, A. Kasama, I. Iwanaga, R. Tanaka and T. Narita, *Oxidation of Metals* **61**, 105 (2004).
4. M. Hara, Y. Matsuda, M. Fukumoto and T. Narita, *Oxidation of Metals* **77**, 295 (2008).
5. T. Abe, N. Sato, M. Fukumoto and M. Hara, *Journal of the Japan Institute of Metals and Materials* **77**, 245 (2013).
6. M. Fukumoto, M. Hara and T. Narita, *Materials Science Forum* **377–384**, 522 (2006).
7. V. Raghavam, *Journal of Phase Equilibria and Diffusion* **27**, 397 (2006).